Science of the Total Environment 851 (2022) 158007

Contents lists available at ScienceDirect

Science of the Total Environment

journal homepage: www.elsevier.com/locate/scitotenv

Quantifying the wet deposition of reactive nitrogen over China: Synthesis of observations and models

Jiani Tan [a,b], Hang Su [b,*], Syuichi Itahashi [c], Wei Tao [b], Siwen Wang [a,b], Rui Li [d], Hongbo Fu [e], Kan Huang [e], Joshua S. Fu [f], Yafang Cheng [a]

[a] Minerva Research Group, Max Planck Institute for Chemistry, Mainz 55128, Germany
[b] Multiphase Chemistry Department, Max Planck Institute for Chemistry, Mainz 55128, Germany
[c] Central Research Institute of Electric Power Industry, Abiko, Chiba 270-1194, Japan
[d] Ministry of Education Key Laboratory for Earth System Modeling, Department of Earth System Science, Tsinghua University, Beijing 100084, China
[e] Shanghai Key Laboratory of Atmospheric Particle Pollution and Prevention (LAP3), Department of Environmental Science and Engineering, Fudan University, Shanghai 200433, China
[f] Department of Civil and Environmental Engineering, University of Tennessee, Knoxville, TN 37996, USA

HIGHLIGHTS

- Monitoring networks of wet N_r deposition (>500 sites) over China are summarized.
- Model capability on predicting wet N_r deposition are evaluated.
- China's wet N_r deposition ranges 7–22 Tg (N) yr^{-1} by different approaches.
- Uncertainties of different estimation approaches are discussed.
- Intergradation of available data (monitoring, satellite and modelling) is suggested.

GRAPHICAL ABSTRACT

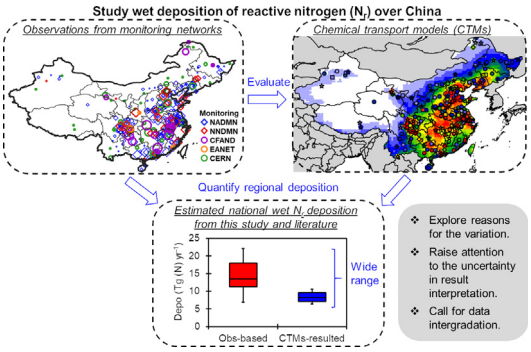

ARTICLE INFO

Editor: Elena Paoletti

Keywords:
Reactive nitrogen
Acid deposition
Site measurement
Model evaluation

ABSTRACT

Accurate estimation on reaction nitrogen (N_r) deposition is highly demanded for assessing the impacts on the environment and human beings. This study investigated the wet deposition of inorganic nitrogen (IN) in mainland China by measurements from over 500 sites from five observational networks/databases and ensemble results of eleven chemical transport models (CTMs). Each data source has its focus and limitations and together formed a comprehensive view over China. But the inconsistency among different sources may hinder the appropriate usage of data. Model evaluation results demonstrated the models' deficiency in simulating the wet NO_3^- deposition over Southeast China (40 % underestimation) and showed an overall underestimation of wet NH_4^+ deposition over the hotspot regions (5–60 % underestimation). A synthesis of this study and twelve reference studies was conducted to quantify the national amount of wet IN deposition. The estimations by CTMs ranged 2.4–3.9 Tg(N) yr^{-1} for wet NO_y deposition and 4–6.7 Tg(N) yr^{-1} for wet NH_x deposition, after adjusting the results with 10–19 % underestimations in wet NO_y deposition and 1–40 % underestimations in wet NH_x deposition. The estimations by ground observations ranged 7.1–9 Tg(N) yr^{-1} for wet NO_y deposition and 8–13.1 Tg(N) yr^{-1} for wet NH_x deposition, which were 20–275 % higher than the estimation by CTMs, but the results were strongly influenced by the abundances and representative of measurements. Studies using statistical techniques to interpolate site observations predicted 3–5.5 Tg(N) yr^{-1} for wet NO_y deposition and 3.9–7.2 Tg(N) yr^{-1} for wet NH_x deposition. This approach benefited from high accuracy and good robustness of the statistical models, but the uncertainty in the interpolation methods could be a potential drawback.

* Corresponding author.
E-mail address: h.su@mpic.de (H. Su).

http://dx.doi.org/10.1016/j.scitotenv.2022.158007
Received 24 May 2022; Received in revised form 4 August 2022; Accepted 9 August 2022
Available online 12 August 2022

1. Introduction

China has witnessed rapid increases in nitrogen (N) deposition from 1980s to 2000s (Liu et al., 2013; Wen et al., 2020; Gu et al., 2015; Cui et al., 2013; Gao et al., 2020). The amount stabilized since then due to the socioeconomic changes in emission control policies (Yu et al., 2019). China is, however, still one of the hotspots of acid deposition over the globe (Tan et al., 2018). It has been widely studied that high deposition that exceeded the natural threshold and resilience could alert the ecosystem (Galloway et al., 2008; Vitousek et al., 1997), leading to acidification and nitrification of the terrestrial and aquatic ecosystems, and therefore causing a series of adverse impacts (Du et al., 2019; Liu et al., 2020). Accurate estimation of the amounts of deposition is thus the essential and fundamental basis to assess the potential influences on the environment and human living.

Long-term site monitoring and chemical transport models (CTMs) are two common approaches to quantify the N_r deposition. Monitoring networks are the important cornerstones. There are several observational networks/datasets for N_r deposition in China. The National Acid Deposition Monitoring Network (NADMN) reports the wet deposition of 320 Chinese cities for 2011–2016 (Li et al., 2019). The Nationwide Nitrogen Deposition Monitoring Network (NNDMN) is a national measurement network established in 2004 by the China Agricultural University (Liu et al., 2011; Yu et al., 2019). It contains the observations of N_r deposition of 32 sites for 2010–2015 (Xu et al., 2019). The Acid and Nutrient Deposition for China's Forest (CFAND) collects data of 56 sites for 1991–2015 from literature (Du, 2018). The Chinese ecosystem research network (CERN), developed in 1988, records the deposition data of 40 sites (Fu et al., 2010). The China Meteorological Administration (CAM) established the Acid Rain Monitoring Network (ARMN) in 1992 and has >300 sites presently (Tang et al., 2010). The Acid Deposition Monitoring Network in East Asia (EANET) is a monitoring network for East Asia developed in 2001. It contains the observations of eleven sites in China since 2000 (https://www.eanet.asia/). Despite the fruitful accumulation of observations, there lacks a platform to provide a high-quality and large-spatial-coverage database of observations, compared to the National Atmospheric Deposition Network (NADP) of North America (http://nadp.slh.wisc.edu/) and the European Monitoring and Evaluation Programme (EMEP) of Europe (https://www.emep.int/).

While monitoring data are acknowledged as revealing the truth, CTMs are praised for imitating the rain-fall process with the physical and chemical mechanisms and full spatial and temporal coverage. Evaluation with the measurement data is required before further analysis, and thus, sufficient amounts of observational data ensure the credibility of the modelling works. Unfortunately, for the large amounts of aforementioned observational datasets in China, only part of them have been used in model evaluation. In global-scale studies and some regional studies, EANET is the only source of observation validation over China (Dentener et al., 2006; Lamarque et al., 2013; Vet et al., 2014; Tan et al., 2018; Wang et al., 2008; Itahashi et al., 2020), where only eleven sites were available. Studies focused on China have used more local datasets, but the spatial coverages are far from satisfactory. Ge et al. (2014) evaluated the NAQPMS model with 31 sites in China from EANET and CMA-ARMN, and the sites were mainly located in Eastern China. Zhao et al. (2017) evaluated the performance of GEOS-Chem over China with about 60 sites from EANET, NNDMN and a local dataset reported by Pan et al. (2012), and the sites were sparsely distributed over China. Ge et al. (2020) used the 83 sites from EANET, CERN, NNDMN and a local dataset to evaluate the performance of nine CTMs over China, and most of the sites were located along the East Coast of China. As a result, there still lacks a comprehensive understanding of the modelling capability in estimating the N_r deposition for entire China.

This study aimed at quantifying the wet deposition of inorganic nitrogen (IN) over mainland China with site measurements and CTMs simulations. First, we collected observations of wet IN deposition from five observational networks/datasets with a total of 521 sites. We compared their spatial coverages and data distributions and discussed the consistencies among different data sources. Then, we evaluated the predictive ability of the ensemble results of eleven CTMs with observations, mainly focusing on five hotspot regions of N_r pollution in China. On this basis, we synthesized the results from this study and twelve reference studies to give estimations on the national amount of wet IN deposition over China.

2. Methods

2.1. Observational database

We collected the ground observations of wet IN deposition around 2010 from 521 monitoring sites over China from literature, including 407 sites from the NADMN network for 2010 (Li et al., 2019), 41 sites from the CERN network for 2013 (Zhu et al., 2015), 32 sites from the NNDMN network for 2010–2015 (former CAUDN network) (Xu et al., 2019), 34 sites from the CFAND version 2.0 database for 2006–2015 (Du, 2018) and 7 sites from the EANET network for 2010.

We ensured the data quality with the following procedures: First, we excluded the sites with <330 days (90 % of a year) of records (based on raining days) to guarantee data completeness. Then, we excluded outliners by the three-sigma rule when multiple monitoring sites from the same network/dataset were located in the same model grids ($0.1^\circ \times 0.1^\circ$). These treatments helped to rule out sites that were less representative than the others and made the model evaluation more reasonable, since the CTMs were not able to reveal the delicate spatial variability of pollutants within one model grid. As a result, about 300 sites were used for model evaluations of wet NO_3^- deposition (341) and wet NH_4^+ deposition (352).

The NO_2 column was derived from version 3.0 NASA Ozone Monitoring Instrument (OMI) products (Krotkov et al., 2017) with an original spatial resolution of $1^\circ \times 1.25^\circ$. The NH_3 column was derived from Infrared Atmospheric Sounding Interferometer (IASA) Level 3 product (Clarisse et al., 2009). We used the average values of year 2010.

2.2. CTMs simulations

The CTMs results came from the second phase of the Task Force on Hemispheric Transport of Air Pollution (HTAP II) (Galmarini et al., 2017). The HTAP was established in 2005 by the United Nations Economic Commission for Europe (UNECE) Convention on Long-range Transboundary Air Pollution (CLRTAP). The major goals are to investigate issues related to climate change and air quality at global scale (http://htap.org/).

We used the multi-model mean (MMM) of eleven global models in the evaluation. The simulations were conducted for the whole year of 2010. The spatial resolution of the MMM is $0.1^\circ \times 0.1^\circ$. Details about the simulations and model set-ups were demonstrated in Tan et al. (2018). The modelled N_r deposition was categorized by NO_y deposition and NH_x deposition. NO_y deposition is the sum of NO_2, HNO_3, NO_3^- and organic nitrates (ON) depositions. The modelled sum of HNO_3 and NO_3^- depositions was evaluated with the observed NO_3^- deposition. NH_x deposition consists of NH_3 and NH_4^+ depositions. The modelled NH_x deposition was assessed by the observed NH_4^+ deposition.

3. Results and discussions

3.1. Inter-comparison of observations from different sources

Fig. 1(a–b) showed the measurement sites of wet NO_3^- and NH_4^+ depositions. The colors of the markers indicated the data sources, and the sizes of the markers indicated the annual accumulated amounts of wet deposition. We defined five regions of focus (demonstrated with colored shades in Fig. 1(a–b)), according to the hotspots of the modelled and observed deposition and the spatial intensities of the monitoring sites. (1) The North China (NC) region included seven provinces/cities in Northeast China. (2) The Yangtze River Delta (YRD) region consisted of four provinces/cities

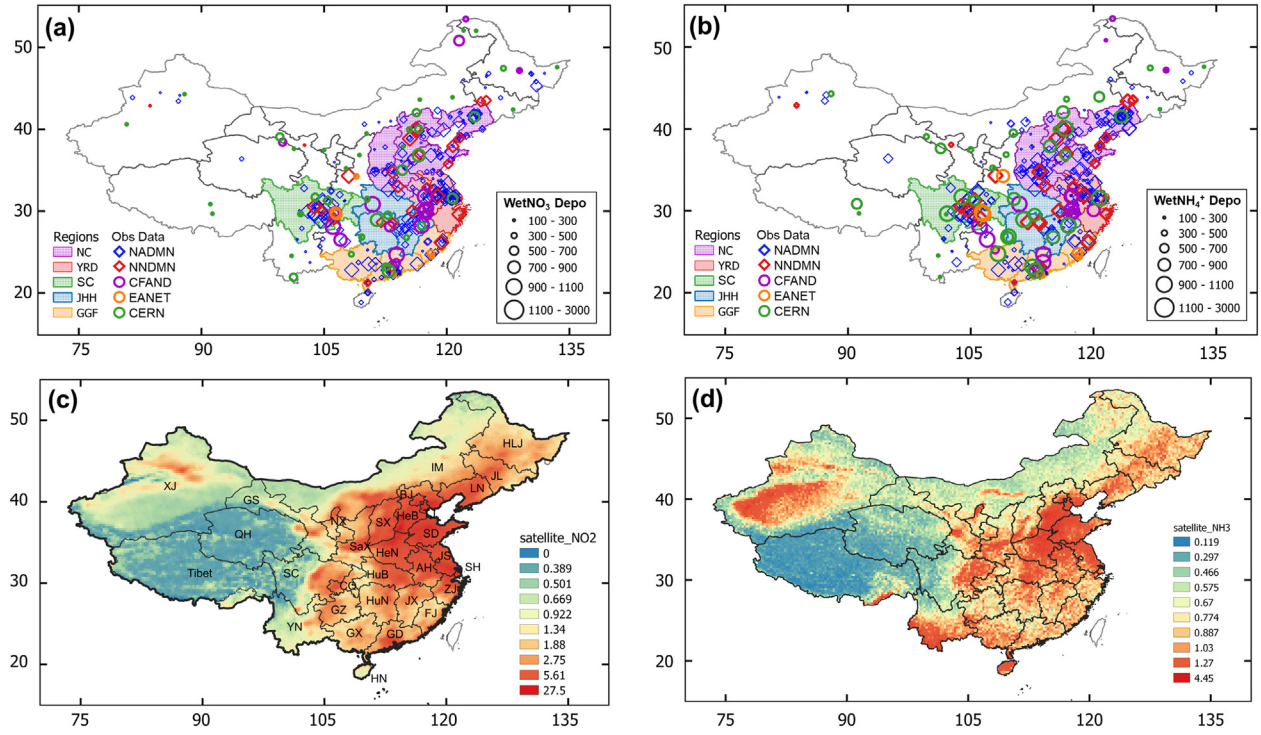

Fig. 1. (a–b) Spatial distributions of measurement sites for wet deposition of (a) NO_3^- and (b) NH_4^+ (unit: mg(N) m^{-2} yr^{-1}). Colored areas were five regions of focus. Colored markers were measurement sites. Colors of the markers indicated the data sources and sizes of the markers indicated the magnitude of depositions. (c–d) Annual average vertical columns of (c) NO_2 and (d) NH_3 by satellite (unit: 10^{15} molecules cm^{-2}).

located on the East Coast of China. (3) The Guangdong (GD, marked in Fig. 1c), Guangxi (GX) and Fujian (FJ) provinces were referred as the GGF region, which was located in the Southeast Coast of China. The NC, YRD and GGF regions were the major economic megalopolises of China. (4) The Sichuan (SC) province and Chongqing (CQ) city were referred as the SC region, which was surrounded by mountains. The basin topography trapped emissions and made this region a hotspot of both air pollutants and acid depositions. (5) The Jiangxi (JX), Hubei (HuB) and Hunan (HuN) provinces were referred as the JHH region, which laid adjoint to the NC, YRD and GGF regions. This region was also observed with high pollution but was less studied due to fewer monitoring sites. The SC, GGF, JHH and southern YRD regions were located in the "Acid Rain Control Area" in the subtropical regions of China, where high acidity was detected in the precipitation (Hao et al., 2000).

The observational database for wet NO_3^- deposition (Fig. 1a) has well covered most of the hotspots demonstrated by the satellite NO_2 column (Fig. 1c), especially the five regions of focus in this study. As for wet NH_4^+ deposition (Fig. 1b), the observational database also had good coverage of the hotspots demonstrated by the satellite NH_3 column (Fig. 1d), except the Xinjiang (XJ) province in Northwest China and Yunnan (YN) province in Southwest China. The NADMN sites, which have been scarcely involved in model evaluations before, were intensively distributed in the hotspot regions and ensured a broad view of these heavily "polluted" regions. On the other hand, the CERN, NNDMN, CFAND and EANET sites were more sparsely distributed. The NNDMN sites were mainly used to evaluate model performances in the NC and GGF regions (Zhao et al., 2017; Ge et al., 2020). The CFAND and CERN networks included several sites in the remote areas that were not covered by the NADMN network, such as the Heilongjiang (HLJ) and Jilin (JL) provinces in Northeast China, Shaanxi (SaX) and Guizhou (GZ) in Center China, and XJ in Northwest China.

Besides the locations of sites, we also compared the data distributions of different datasets (Fig. 2). The average of the CERN sites was the closest to the overall average for both wet NO_3^- deposition and wet NH_4^+ deposition, but all the observations were below 2000 (NO_3^-) and 3000 (NH_4^+) mg (N) m^{-2} yr^{-1}, so that the extreme high deposition fluxes may not be sampled by the sites of this network. The observations at the NNDMN and CFAND sites were overall higher than the others. The range of the EANET dataset was much smaller than the others, suggesting that this widely used observational network in global studies (Dentener et al., 2006; Lamarque et al., 2013; Vet et al., 2014; Tan et al., 2018; Wang et al., 2008; Itahashi et al., 2020) can merely reveal partial of the condition in China.

The representativeness of the sites was also affected by their land-use types (LUTs). Fig. 2(b) and (d) summarized the observed wet depositions at sites on urban, rural (agriculture), background (forest and grassland) and others (coastal, desert, etc.) LUTs by different datasets. About 85 % of the sites were located on urban and rural LUTs, indicating that the measurements mainly revealed the N_r deposition conditions under human impacts. The observed wet NO_3^- depositions were higher at urban sites (832.0 mg(N) m^{-2} yr^{-1}) than rural (680.3 mg(N) m^{-2} yr^{-1}) and background (757.0 mg(N) m^{-2} yr^{-1}) sites, agreed with the trends of N_r species in the atmosphere (Wen et al., 2020). On the other hand, the wet NH_4^+ depositions at rural sites (836.3 mg(N) m^{-2} yr^{-1}) were comparable to those at urban sites (884.1 mg(N) m^{-2} yr^{-1}), owing to the agricultural NH_3 emissions. The EANET and CERN datasets presented the opposite orders among different LUTs (i.e. urban < rural for wet NO_3^- deposition) due to small sample sizes. The NADMN dataset was short of information for background regions, and the CFAND dataset, conversely, only focused on background regions. The observations from the NNDMN dataset were overwhelmingly higher than the other datasets at both urban and rural sites, due to that most sites were located in intensively polluted regions.

The assemble of datasets could offer more information than individuals, but problems were found when merging these datasets. We noticed that the observations could differ largely among nearby sites that come from different data sources. For instance, one urban site from NNDMN in the SC province valued 1700 mg(N) m^{-2} yr^{-1} and the four adjoining urban sites from NADMN all valued <700 mg(N) m^{-2} yr^{-1} (Fig. 1a). Similarly, the observations from NADMN sites doubled those from the adjacent CERN sites in the Hebei (HeB), Beijing (BJ) and JX provinces. The inconsistency could come from lacking standard sampling and quality checking procedures in the

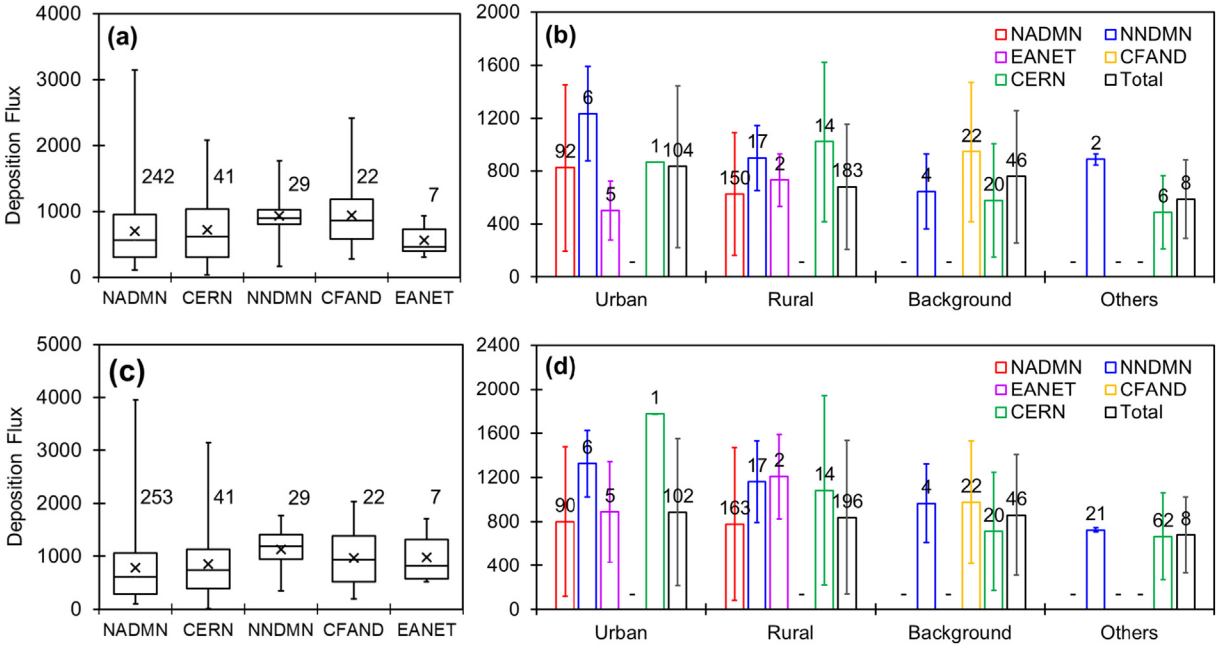

Fig. 2. (a) Boxplot of observed wet deposition of NO_3^- and (b) average and standard deviation of observed wet deposition of NO_3^- at sites on different land-use types (unit: mg (N) m^{-2} yr^{-1}). (c–d) Same as (a–b) but for wet deposition of NH_4^+. Number above the bars indicated the numbers of sites in the categories.

measuring process (He et al., 2015). Despite the fruitful monitoring works reported in previous publications (Du, 2018; Fu et al., 2010; Li et al., 2019; Tang et al., 2010; Xu et al., 2019; Yu et al., 2019), there lacks a platform to function not only as a synthesis of data but also for strict control of data quality to warrant further analysis and applications.

3.2. Model performance on wet deposition

3.2.1. Model performance over the hotspot regions

Figures. 3–4 and Tables 1–2 showed the model performance on simulating the annual accumulated amount of wet NO_3^- and NH_4^+ depositions. The Normalized Mean Bias (NMB) indicated the model's accuracy in catching the general value. The Pearson correlation coefficient (r) elucidated the percentage of observations explained by models. The Fraction of modelled values within ±50 % of observations (FAC2) indicated the model's ability in covering the extreme values.

The overall performance on wet NO_3^- deposition was acceptable with NMB of (−10 %) and FAC2 of 59 % (Fig. 3b). Among the five regions of focus in this study, the SC region was generally well simulated with NMB of (−10 %) and FAC2 of 72 % (Table 1). The NMB values at the YRD (8 %) and NC (17 %) regions were acceptable, but the FAC2 values (around 50 %) were below average. The models overestimated the wet NO_3^- deposition at almost one-third of the sites in the NC and YRD regions by a factor of two (Fig. 3b) and most of the overestimated sites were rural sites (Fig. 3c). The performance on the NO_3^- ions concentration in precipitation was better (Fig. 3e). Evaluation on the precipitation also confirmed the positive model errors on simulating rain fall, especially on low values (<400 mm yr^{-1}) (Fig. 3h). Adjusting precipitation with site observations and satellite products was found an effective way to improve model accuracy on wet deposition (Itahashi et al., 2021). On the contrary, the JHH region was underestimated by 27 %, but the FAC2 (78 %) was the highest among all region. The observations at background sites were concentrated at around 1000 mg(N) m^{-2} and the model had well reproduced this pattern. The bias came from the underestimation at rural and urban sites. The model performance in the GGF region was the worst among the five with both large NMB (−40 %) and low FAC2 (53 %). About one-fourth of the sites in the GGF region were underestimated in the amount of wet NO_3^- deposition by a factor of two (Fig. 3b). Sites of all LUTs were underestimated, especially the urban sites with observations higher than 1000 mg(N) m^{-2}. Fig. 3d showed that sites in the GD province were generally well predicted, but some sites in the GX province were severely underestimated.

Wet NH_4^+ deposition was generally underestimated by 31 % and the overall FAC2 value was only 48 % (Fig. 4). All five regions of focus expect YRD were largely underestimated by 20–60 %. The SC, JHH and NC regions have similar NMB values [−(20–30 %)] and FAC2 values (50–60 %). The YRD region has low NMB (−5 %) and FAC2 (35 %) values. Despite the broad underestimations in these three regions, about one-third of the sites at the NC, YRD and JHH regions were overestimated by a factor of two (Fig. 4b). And same levels of biases were found in the NH_4^+ ion concentration in precipitation (Fig. 4e). The model has the worst performance in the GGF region, similar to its performance on wet NO_3^- deposition. About half of the sites in the GGF region were underestimated by a factor of two in both the amount of deposition and ion concentration (Fig. 4(b) and (e)).

The model has higher biases at rural sites than urban sites. The rural sites received ranged transport of air pollutants from urban emissions, which could contribute substantially to the pollution (Chen et al., 2017). Simulation of such process in the CTMs were driven by many factors including emission sources, meteorological factors and transformations of pollutants. Thus, modelling of rural sites involved more uncertainty than urban sites. In addition, the CTMs provided estimations at a regional scale, with model grids covering both urban and rural areas. Model simulations with coarse grids could fail to distinct the concentration gradients from urban sites to rural sites.

Our results have similar R and FAC2 values with the model evaluation work by Ge et al. (2020) in both wet NO_3^- deposition and wet NH_4^+ deposition, but worse R and NMB values than Zhao et al. (2017) in wet NH_4^+ deposition (Table 2). Zhao et al. (2017) used the same emission inventory as this study from the Multi-resolution Emission Inventory for China (MEIC) (Li et al., 2017) but replaced the NH_3 emission with the Regional Emission in Asia (REAS-v2), which estimated higher NH_3 emissions than MEIC. However, their simulation in the SC region showed an overall high deposition at around 1600–2500 mg(N) m^{-2} yr^{-1}, while our 41 observations in this region ranged 600–1500 mg(N) m^{-2} yr^{-1}, which indicated the possibility of over-adjustment in the emission.

Evaluation of the dissolved ON (DON) was not included in this study. DON contributed to only 2–3 % of the total N_r deposition (ON + IN) in the model results, much lower than the 23–28 % reported by observational

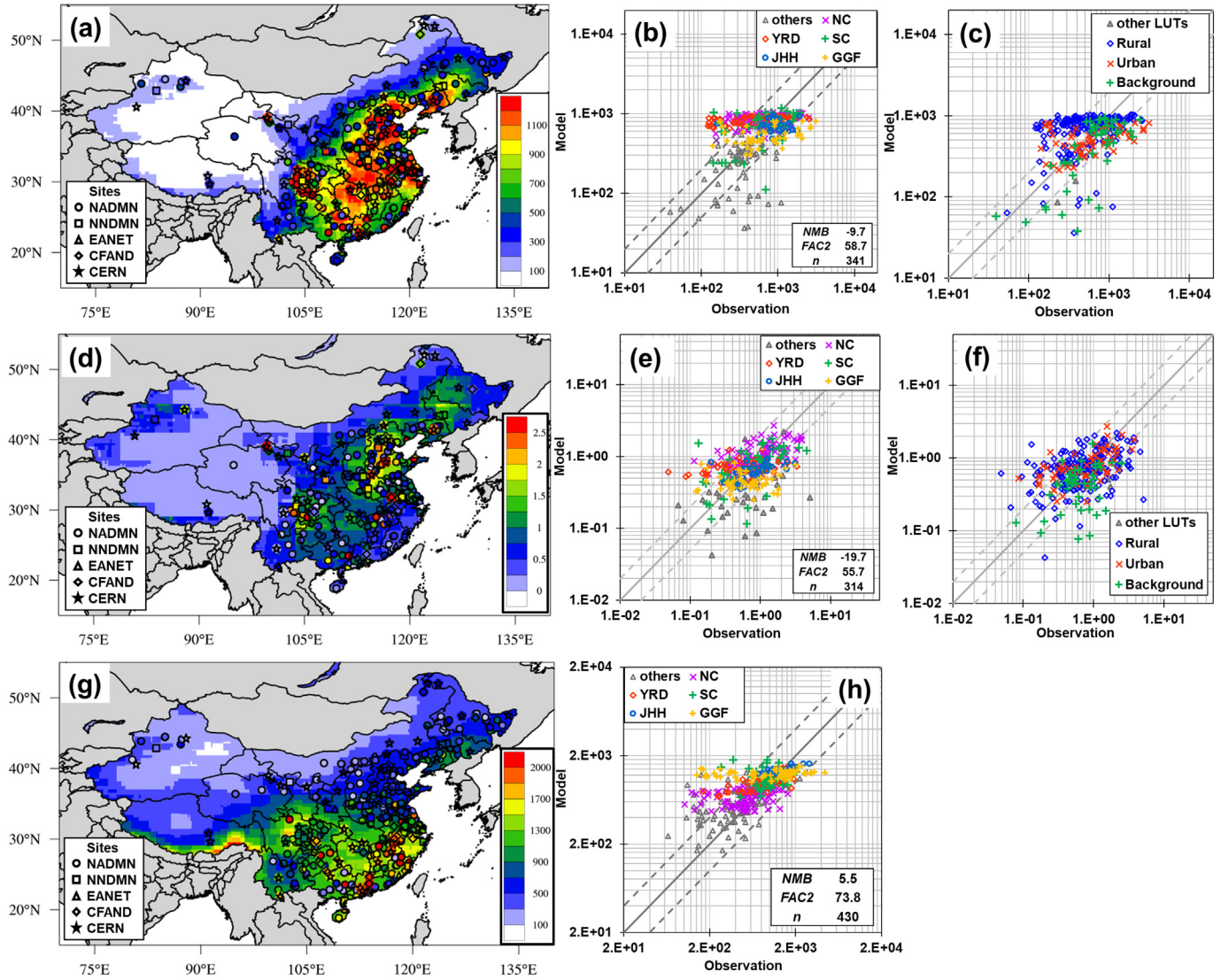

Fig. 3. Model performance on annual accumulated wet NO_3^- deposition and precipitation. (a) Modelled wet deposition (contours) compared with observations (markers) (unit: mg(N) m^{-2} yr^{-1}). Scatter plot of the modelled and observed wet NO_3^- deposition (b) in different regions (defined in Fig. 1) and (c) on different land-use types. (d–f) Same as (a–c) but for NO_3^- ion in precipitation (unit: mg(N) L^{-1}). (g–h) Same as (a–b) but for precipitation (unit: mm yr^{-1}). Notes for the statistic indexes: NMB — normalized mean bias, FAC2 — fraction of model results within ±50 % of observation, n — numbers of sites used for evaluation.

evidence in China (Zhang et al., 2012; Jiang et al., 2013). Severe underestimation of DON in wet deposition was anticipated. However, DON were not involved in the routine monitoring network of wet deposition (Walker et al., 2019), and the methods of measurements were of high uncertainties (Cape et al., 2011; Neff et al., 2002; Walker et al., 2012). Further study on the monitoring and modelling of DON deposition were strongly recommended.

3.2.2. Model performance on monthly variations

Fig. 5 showed the modelled and observed monthly variations of wet NO_3^- and NH_4^+ depositions. The red lines represented the average values of all sites and the boxplots indicated the ranges. For wet NO_3^- deposition, the observations (Fig. 5(a) red line) peaked in Summer with a small peak in February and were generally low in Fall. The model (Fig. 5(b) red line) caught this trend and reproduced the magnitude of the peak in Summer at ~100 mg (N) m^{-2} mon^{-1}. The modelled values were close to the observations during Summer with only 3–7 % differences but were higher than the observations in the other months by 20–40 %. For wet NH_4^+ deposition, both observed (Fig. 5(c)) and modelled (Fig. 5(d)) depositions showed one single peak in Summer, but the peaking value was underestimated by 30 % by the model. In the other seasons, the modelled values agreed well with the observations (NMB < 10 %).

The model performance on the spatial variations among sites were implied by the interquartile range, calculated as the difference between the 3rd quantile and 1st quantile of the boxplot. The observed NO_3^- depositions displayed large interquartile ranges of 60–100 mg (N) m^{-2} mon^{-1} in all seasons except winter (~40 mg (N) m^{-2} mon^{-1}). While, the modelled depositions showed smaller spatial variations in all seasons (30–50 mg (N) m^{-2} mon^{-1}) except Summer (~100 mg (N) m^{-2} mon^{-1}). Similar problem was also found in wet NH_4^+ deposition. The models performed well in the temporal variations but were weak at the spatial dispersions of data.

3.3. Synthesis of studies on the wet IN deposition over China

Table 3 summarized the national amounts of wet IN deposition over China calculated by this study and by literature. For the purpose of cross-comparison, we only listed the studies that included estimations around the year 2010.

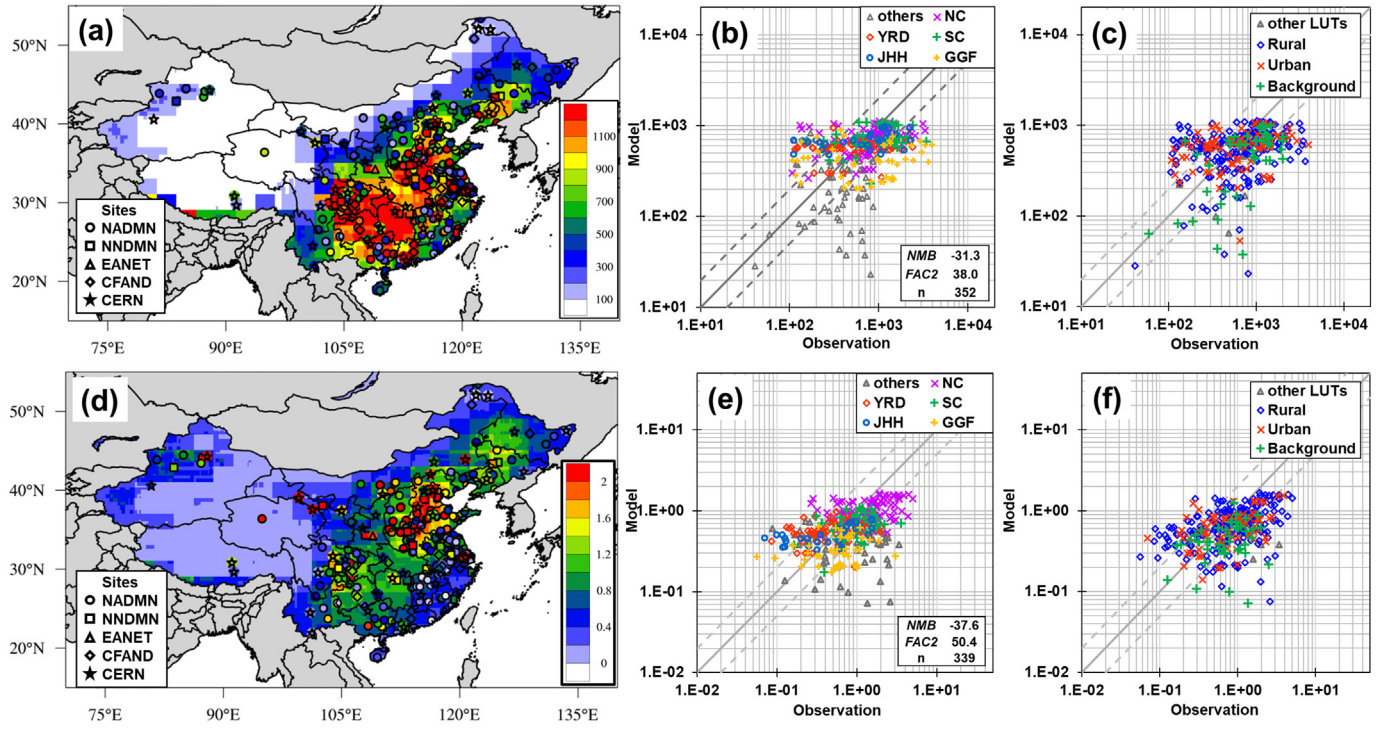

Fig. 4. Same as Fig. 3 but for the (a–c) wet NH_4^+ deposition (unit: mg(N) m^{-2} yr^{-1}) and (d–f) NH_4^+ ion in precipitation (unit: mg(N) L^{-1}).

Estimations by different CTMs studies (Table 3, studies 1–4) ranged 2.5–3.4 Tg(N) yr^{-1} for wet NO_y deposition and 3.1–6.6 Tg(N) yr^{-1} for wet NH_x deposition. According to Table 1, all studies except study 3 have underestimated the wet NO_3^- deposition by 10–19 %, and all studies have underestimated the wet NH_4^+ deposition by 1–40 %. After adjusting the national amounts with these biases, the range of estimations (as shown in the parentheses in Table 3) changed to 2.4–3.9 Tg(N) yr^{-1} for NO_y deposition and 4–6.7 Tg(N) yr^{-1} for NH_x deposition. The differences among studies came from the treatments of both model inputs and outputs. All studies used the same emission inventory for NO_x (Li et al., 2017) and had close estimations on wet NO_y deposition. Zhao et al. (2017) estimated a higher wet NH_x deposition than the other three, due to using a different emission inventory for NH_3 as discussed in Section 3.1. Gao et al. (2020) also found that using an updated emission inventory could largely improve the model performance in China. In addition, using different precipitation was an important source of inter-model differences (Itahashi et al., 2020). Ge et al. (2020), Itahashi et al. (2020) and this study used the ensemble results of multiple models, which have been proven to have advantage over single model studies in providing robust results on quantification (Wang et al., 2008; Vivanco et al., 2018; Tan et al., 2018; Yoshioka et al., 2019). The estimation by this study was apparently higher than the other two ensemble results. This study excluded the unreasonable results from the ensemble for the purpose of accurate quantification of deposition amount (Tan et al., 2018). While Ge et al. (2020) and Itahashi et al. (2020) aimed at evaluating the predictive abilities of different models, thus all participating models were kept for comparison.

For studies that reported the statistics of observational datasets (Table 3, studies 5–8), the national total depositions were estimated by multiplying the average deposition of the measurement sites by the area of mainland China. The estimated wet NO_y deposition ranged 7.1–9 Tg(N) yr^{-1} and wet NH_x deposition ranged 8–13.1 Tg(N) yr^{-1}. The estimations by Liu et al. (2013), Xu et al. (2015) and Wen et al. (2020) were higher than those by this study by 11–21 % on wet NO_y deposition and 18–39 % on wet NH_x deposition. These three studies all used the NNDMN dataset, which generally revealed the condition in highly polluted regions (Fig. 1a) and the observed values were generally higher than the other datasets (Fig. 2(b) and (d)). This study included more observations in remote areas than the NNDMN dataset so that the estimations on the national amounts were lower. The abundance and representative of the measurements, as discussed in Section 3.1, could affect the estimations vastly.

Table 1
Model evaluation studies for wet NO_3^- deposition.

Projects/models	Reference	Observational networks (number of sites)	Regions	Mean of observation (mg(N) m^{-2} yr^{-1})	Mean of model (mg(N) m^{-2} yr^{-1})	r	NMB (%)	FAC2 (%)
HTAP II Ensemble	This study	MIX (n = 43)	SC	816.5	731.3	0.5	−10.4	72.1
		MIX (n = 32)	JHH	996.9	727.1	0.0	−27.1	78.1
		MIX (n = 64)	YRD	775.4	837.0	0.4	7.9	51.6
		MIX (n = 83)	NC	715.8	840.2	0.3	17.4	47.0
		MIX (n = 49)	GGF	896.9	540.5	0.4	−39.7	53.1
		MIX (n = 70)	Others	436.2	311.8	0.5	−28.5	65.7
		All sites (n = 341)		734.7	663.7	0.3	−9.7	58.7
MICS-Asia III Ensemble[1]	Ge et al., 2020	EANET, CERN, NNDMN, DEE (n = 83)	Over whole China	640.0	677.8	0.2–0.4[2]	5.9	36–60[2]
GEOS-Chem	Zhao et al., 2017	EANET, NNDMN, 10 sites in NC (n = 87)		–	–	0.7	−15.0	–
MICS-Asia III Ensemble[1]	Itahashi et al., 2020	EANET (n = 54)	East Asia	347.5	282.6	0.4	−18.7	46.8
HTAP II Ensemble	Tan et al., 2018	EANET (n = 43)		356.4	355.7	0.7	−0.2	76.7

[1] Model Inter-comparison Study for Asia (MICS-Asia) phase III.
[2] Range of results from multiple models.

Table 2
Model evaluation studies for wet NH_4^+ deposition.

Projects/models	Reference	Observational networks (number of sites)	Regions	Mean of observation (mg(N) m^{-2} yr^{-1})	Mean of model (mg(N) m^{-2} yr^{-1})	r	NMB (%)	FAC2 (%)
HTAP II Ensemble	This study	MIX (n = 41)	SC	1119.8	770.6	0.2	−31.2	61.0
		MIX (n = 32)	JHH	874.3	697.9	0.4	−20.2	53.1
		MIX (n = 66)	YRD	614.3	585.3	0.1	−4.7	34.9
		MIX (n = 95)	NC	970.0	717.0	0.4	−26.1	66.3
		MIX (n = 50)	GGF	1095.8	430.6	0.2	−60.7	22.0
		MIX (n = 68)	Others	493.5	300.4	0.4	−39.1	44.1
		All sites (n = 352)		837.9	575.7	0.3	−31.3	48.0
MICS-Asia III Ensemble[1]	Ge et al., 2020	EANET, CERN, NNDMN, DEE (n = 83)	Over whole China	1010.0	612.2	0.2–0.5[2]	−39.4	19-63[2]
GEOS-Chem	Zhao et al., 2017	EANET, NNDMN, 10 sites in NC (n = 87)		–	–	0.6	−1.0	–
MICS-Asia III Ensemble[1]	Itahashi et al., 2020	EANET (n = 54)	East Asia	440.7	378.3	0.4	−14.2	38.0
HTAP II Ensemble	Tan et al., 2018	EANET (n = 43)		534.5	505.8	0.7	−5.4	60.5

[1] Model Inter-comparison Study for Asia (MICS-Asia) phase III.
[2] Range of results from multiple models.

To overcome the weakness in establishing spatial correlation for observation-based estimations, recent studies (Table 3, studies 9–14) used various geo-spatial statistical approaches to interpolate the observations, including Kriging (Zhu et al., 2015; Yu et al., 2019), geographical weighting regression (Li et al., 2019) and constrain with satellite products (Liu et al., 2017; Liu et al., 2021; Li et al., 2020). The estimated wet NO_y deposition ranged 3–5.5 Tg(N) yr^{-1} and wet NH_x deposition ranged 3.9–7.2 Tg (N) yr^{-1}. This pathway took the advantage of low requirement of computational resources (Reinstorf et al., 2005), but the estimations were unstable and incomparable among different studies. Even studies with the same interpolation methods could result in very different predictions, not to mention those with different methods. Zhu et al. (2015) and Yu et al. (2019) both adopted the Kriging interpolation, but their products differed by 32 % on wet NO_y deposition and 16 % on wet NH_x deposition. Liu et al. (2021) and Li et al. (2020) both interpolated site observations with satellites to construct the wet NH_x deposition field, but their estimations differed by 16 %. There is a lack of studies to manage the degree of uncertainty of this approach. The variance of Kriging interpolation ranged 12–100 % in the study by Holland et al. (2005) over the United States and Western Europe and ranged 9 %–56 % in the study by Lü and Tian (2007) over China. In addition, the spatial patterns of wet N deposition, especially NH_x, showed a fast decrease with distance to the emission sources (Du et al., 2014), which indicated high risk when the spatial interpolation was operated on limited number of sites (Liu et al., 2015). The high variability could offset the benefit brought by the high accuracy and good robustness of the statistical models.

4. Conclusions

This study investigated the wet IN deposition over mainland China with site measurements and CTMs. We collected a database from five observational networks/datasets of NADMN (407 sites), CERN (41 sites), NNDMN (32 sites), CFAND (34 sites) and EANET (7 sites). The NADMN sites were intensively distributed in the hotspot regions of N_r pollution. The NNDMN sites were mainly located in the NC and GGF regions and revealed more of the conditions in the highly polluted regions. The CERN, CFAND and EANET sites were sparsely located over China, with several sites in the remote areas. The EANET sites were the most widely used dataset in previous model evaluation studies in East Asia, but were unable to represent the condition in China. The majority of the sites (85 %) were located in urban and rural regions, and less information was provided for remote and background regions (i.e. forest and grassland).

We used this database to evaluate the performance of the ensemble of eleven CTMs from HTAP II. Wet NO_3^- deposition was generally well simulated over China (MB = −10 %) and in the SC (−10 %), YRD (8 %) and NC (17 %) regions, but was underestimated in the JHH (27 %) and GGF

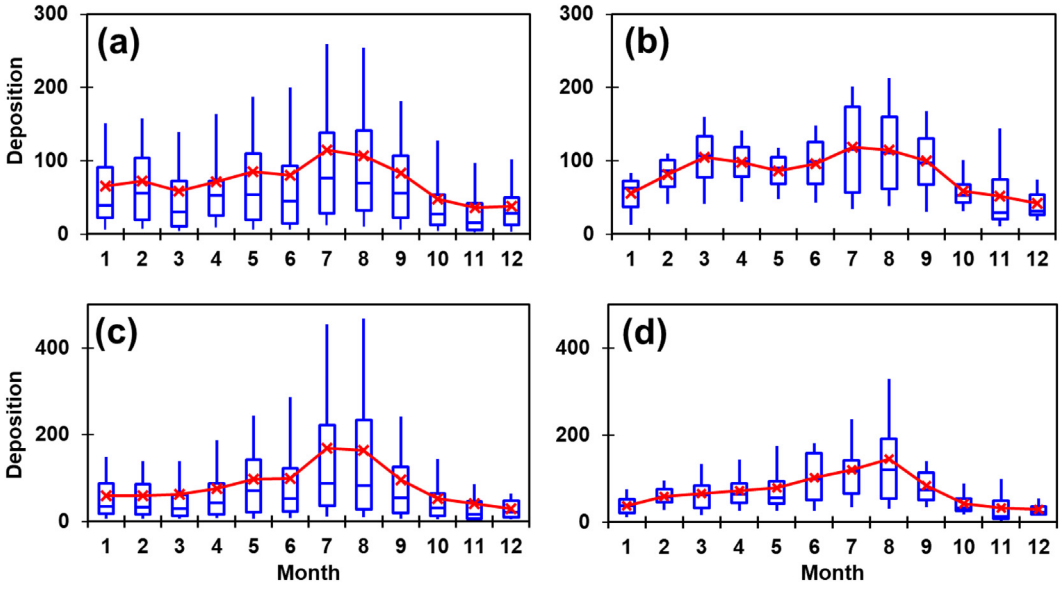

Fig. 5. Monthly variations of (a) observed and (b) modelled wet NO_3^- deposition, and (c) observed and (d) modelled wet NH_4^+ deposition (unit: mg(N) m^{-2} mon^{-1}). Red line indicated the average values of all sites.

Table 3
Estimations on national amount of wet IN deposition in China (unit: Tg(N) yr^{-1}).

Study no.	Type of studies	Reference	Methods	Study period	Wet NO_y	Wet NH_x
1	CTMs	This study	Multi-model ensemble from HTAP-II	2010	3.4 (3.8)*	4.2 (5.5)*
2		Itahashi et al., 2020	Multi-model ensemble from MICS-Asia-III	2010	2.5 (3.0)*	3.5 (4.0)*
3		Ge et al., 2020		2010	2.5 (2.4)*	3.1 (4.3)*
4		Zhao et al., 2017	GEOS-Chem	2008–2012	3.4 (3.9)*	6.6 (6.7)*
5	Observations	Liu et al., 2013	About 30 NNDMN sites	2010	9	13.1
6		Wen et al., 2020	66 NNDMN sites	2011	8	10
7		Xu et al., 2015	43 NNDMN sites	2010–2014	8.6	9.8
8		This study	About 350 sites from different sources	2010	7.1	8.0
9	Observations with geo-spatial techniques	Zhu et al., 2015	41 CERN sites with Kriging interpolation	2013	5.4	6.6
10		Yu et al., 2019	260 sites with Kriging interpolation	2011–2015	4.1	5.7
11		Li et al., 2019	1282 NADMN sites with geographical weighting regression	2011	3	3.9
12		Li et al., 2020	500 NADMN sites interpolated with satellite products	2011–2016	–	7.2
13		Liu et al., 2021	43 NNDMN sites interploated with satellite products	2008–2016	–	6.2
14		Liu et al., 2017	33 NNDMN sites interpolated with satellite products	2010–2012	5.5	–

* Values in the parentheses were the adjusted results with model bias from evaluation.

(40 %) regions. The large underestimation in the GGF region came from bias in the NO_3^- ions in precipitation. Wet NH_4^+ deposition was general underestimated over China by 31 %, and was somewhat underestimated in all five hotspot-regions by 5–60 %. The bias mainly came from the NH_4^+ ion concentration in precipitation. The CTMs had more difficulties and uncertainties in simulating the N_r deposition at rural sites than urban sites.

We synthesized the estimated national amounts of wet IN deposition over China by this study and twelve reference studies. CTMs studies generally have 6–19 % underestimation in wet NO_3^- deposition and 1–40 % underestimation in wet NH_4^+ deposition. After adjusting the results with the biases, the estimations ranged 2.4–3.9 Tg(N) yr^{-1} for wet NO_y deposition and 4–6.7 Tg(N) yr^{-1} for wet NH_x deposition. Treatment of both model inputs and outputs contributed to the differences among studies. Estimations from observational databases ranged 7.1–9 Tg(N) yr^{-1} for wet NO_y deposition and 8–13.1 Tg(N) yr^{-1} for wet NH_x deposition, which were 20–275 % higher than the estimations by CTMs. This approach was largely affected by the abundances and representative of measurements. Studies used statistical approaches to interpolate site observations to overcome the shortage of observations and to develop geo-correlation among sites. The estimated wet NO_y deposition ranged 3–5.5 Tg(N) yr^{-1} and wet NH_x deposition ranged 3.9–7.2 Tg(N) yr^{-1}. The estimations by this approach were unstable, despite the high accuracy and good robustness of the statistical models.

This study aimed at contributing to a better understanding of N_r deposition in China, one of the world's fastest-growing economies. The datasets from different sources, including various monitoring networks and modelling results, together could offer more information than single one. However, large inconsistencies among them may discourage the usage, and study on data integration is strongly recommended. This study is a pioneer practice of the measurement-model fusion of Global Total Atmospheric Deposition (MMF-GTAD) project initialed by the World Meteorological Organization's Global Atmosphere Watch Programme (WMO GAW) (Fu et al., 2022). Future study will continue to improve our understanding on atmospheric deposition and N_r budget and the impacts on human beings. This study provides broad-scale estimation of wet N_r deposition on the ecosystem. The data could also help local-scale study on the environmental impacts with calibration experiments (Jung and Kim, 2017; Gao et al., 2020).

CRediT authorship contribution statement

Jiani Tan: Conceptualization, Formal analysis, Visualization, Writing – original draft. **Hang Su:** Supervision, Conceptualization, Formal analysis, Writing – review & editing. **Syuichi Itahashi:** Resources, Writing – review & editing. **Wei Tao:** Investigation, Writing – review & editing. **Siwen Wang:** Resources, Writing – review & editing. **Rui Li:** Resources, Writing – review & editing. **Hongbo Fu:** Resources, Writing – review & editing. **Kan Huang:** Resources, Writing – review & editing. **Joshua S. Fu:** Conceptualization, Writing – review & editing. **Yafang Cheng:** Supervision, Conceptualization, Formal analysis, Writing – review & editing.

Data availability

Data will be made available on request.

Declaration of competing interest

The authors declare that they have no known competing financial interests or personal relationships that could have appeared to influence the work reported in this paper.

Acknowledgements

This study is supported by the Max Planck Society (MPG). Y.C. acknowledges the Minerva Program of MPG.

References

Cape, J.N., Cornell, S.E., Jickells, T.D., Nemitz, E., 2011. Organic nitrogen in the atmosphere - where does it come from?A review of sources and methods. Atmos. Res. 102, 30–48. https://doi.org/10.1016/j.atmosres.2011.07.009.

Chen, D.S., Liu, X.X., Lang, J.L., Zhou, Y., Wei, L., Wang, X.T., Guo, X.R., 2017. Estimating the contribution of regional transport to PM2.5 air pollution in a rural area on the North China Plain. Sci. Total Environ. 583, 280–291. https://doi.org/10.1016/j.scitotenv.2017.01.066.

Clarisse, L., Clerbaux, C., Dentener, F., Hurtmans, D., Coheur, P.F., 2009. Global ammonia distribution derived from infrared satellite observations. Nat. Geosci. 2, 479–483. https://doi.org/10.1038/ngeo551.

Cui, S., Shi, Y., Groffman, P.M., Schlesinger, W.H., Zhu, Y.G., 2013. Centennial-scale analysis of the creation and fate of reactive nitrogen in China (1910–2010). Proc. Natl. Acad. Sci. U. S. A. 110, 2052–2057. https://doi.org/10.1073/pnas.1221638110.

Dentener, F., Drevet, J., Lamarque, J.F., Bey, I., Eickhout, B., Fiore, A.M., Hauglustaine, D., Horowitz, L.W., Krol, M., Kulshrestha, U.C., Lawrence, M., Galy-Lacaux, C., Rast, S., Shindell, D., Stevenson, D., Van Noije, T., Atherton, C., Bell, N., Bergman, D., Butler, T., Cofala, J., Collins, B., Doherty, R., Ellingsen, K., Galloway, J., Gauss, M., Montanaro, V., Muller, J.F., Pitari, G., Rodriguez, J., Sanderson, M., Solmon, F., Strahan, S., Schultz, M., Sudo, K., Szopa, S., Wild, O., 2006. Nitrogen and sulfur deposition on regional and global scales: a multimodel evaluation. Glob. Biogeochem. Cycles 20, 21. https://doi.org/10.1029/2005gb002672.

Du, E., Jiang, Y., Fang, J.Y., de Vries, W., 2014. Inorganic nitrogen deposition in China's forests: status and characteristics. Atmos. Environ. 98, 474–482. https://doi.org/10.1016/j.atmosenv.2014.09.005.

Du, E., 2018. Data descriptor: a database of annual atmospheric acid and nutrient deposition to China's forests. Sci. Data 5, 1–6. https://doi.org/10.1038/sdata.2018.223.

Du, E., Fenn, M.E., De Vries, W., Ok, Y.S., 2019. Atmospheric nitrogen deposition to global forests: status, impacts and management options. Environ. Pollut. 250, 1044–1048. https://doi.org/10.1016/j.envpol.2019.04.014.

Fu, B.J., Li, S.G., Yu, X.B., Yang, P., Yu, G.R., Feng, R.G., Zhuang, X.L., 2010. Chinese ecosystem research network: progress and perspectives. Ecol. Complex. 7, 225–233. https://doi.org/10.1016/j.ecocom.2010.02.007.

Fu, J.S., Carmichael, G.R., Dentener, F., Aas, W., Andersson, C., Barrie, L.A., Cole, A., Galy-Lacaux, C., Geddes, J., Itahashi, S., Kanakidou, M., Labrador, L., Paulot, F., Schwede, D., Tan, J., Vet, R., 2022. Improving estimates of sulfur, nitrogen, and ozone total deposition through multi-model and measurement-model fusion approaches. Environ. Sci. Technol. 56, 2134–2142. https://doi.org/10.1021/acs.est.1c05929.

Galloway, J.N., Townsend, A.R., Erisman, J.W., Bekunda, M., Cai, Z.C., Freney, J.R., Martinelli, L.A., Seitzinger, S.P., Sutton, M.A., 2008. Transformation of the nitrogen cycle: recent trends, questions, and potential solutions. Science 320, 889–892. https://doi.org/10.1126/science.1136674.

Galmarini, S., Koffi, B., Solazzo, E., Keating, T., Hogrefe, C., Schulz, M., Benedictow, A., Griesfeller, J.J., Janssens-Maenhout, G., Carmichael, G., Fu, J., Dentener, F., 2017. Technical note: coordination and harmonization of the multi-scale, multi-model activities HTAP2, AQMEII3, and MICS-Asia3: simulations, emission inventories, boundary conditions, and model output formats. Atmos. Chem. Phys. 17, 1543–1555. https://doi.org/10.5194/acp-17-1543-2017.

Gao, Y., Zhou, F., Ciais, P., Miao, C.Y., Yang, T., Jia, Y.L., Zhou, X.D., Klaus, B.B., Yang, T.T., Yu, G.R., 2020. Human activities aggravate nitrogen-deposition pollution to inland water over China. Natl. Sci. Rev. 7, 430–440. https://doi.org/10.1093/nsr/nwz073.

Ge, B., Itahashi, S., Sato, K., Xu, D., Wang, J., Fan, F., Tan, Q., Fu, J.S., Wang, X., Yamaji, K., Nagashima, T., Li, J., Kajino, M., Liao, H., Zhang, M., Wang, Z., Li, M., Woo, J.-H., Kurokawa, J., Pan, Y., Wu, Q., Liu, X., Wang, Z., 2020. Model inter-comparison study for Asia (MICS-Asia) phase III: multimodel comparison of reactive nitrogen deposition over China. Atmos. Chem. Phys. 20, 10587–10610. https://doi.org/10.5194/acp-20-10587-2020.

Ge, B.Z., Wang, Z.F., Xu, X.B., Wu, J.B., Yu, X.L., Li, J., 2014. Wet deposition of acidifying substances in different regions of China and the rest of East Asia: modeling with updated NAQPMS. Environ. Pollut. 187, 10–21. https://doi.org/10.1016/j.envpol.2013.12.014.

Gu, B.J., Ju, X.T., Chang, J., Ge, Y., Vitousek, P.M., 2015. Integrated reactive nitrogen budgets and future trends in China. Proc. Natl. Acad. Sci. U. S. A. 112, 8792–8797. https://doi.org/10.1073/pnas.1510211112.

Hao, J.M., Wang, S.X., Liu, B.J., He, K.B., 2000. Designation of acid rain and SO2 control zones and control policies in China. J. Environ. Sci. Health Pt A-Toxic/Hazard. Subst. Environ. Eng. 35, 1901–1914. https://doi.org/10.1080/10934520009377085.

He, N., Zhu, J., Wang, Q., 2015. Uncertainty and perspectives in studies of atmospheric nitrogen deposition in China: a response to Liu et al. (2015). Sci. Total Environ. 520, 302–304. https://doi.org/10.1016/j.scitotenv.2015.03.063.

Holland, E.A., Braswell, B.H., Sulzman, J., Lamarque, J.F., 2005. Nitrogen deposition onto the United States and Western Europe: synthesis of observations and models. Ecol. Appl. 15, 38–57. https://doi.org/10.1890/03-5162.

Itahashi, S., Ge, B.Z., Sato, K., Fu, J.S., Wang, X.M., Yamaji, K., Nagashima, T., Li, J., Kajino, M., Liao, H., Zhang, M.G., Wang, Z., Li, M., Kurokawa, J., Carmichae, G.R., Wang, Z.F., 2020. MICS-Asia III: overview of model intercomparison and evaluation of acid deposition over Asia. Atmos. Chem. Phys. 20, 2667–2693. https://doi.org/10.5194/acp-20-2667-2020.

Itahashi, S., Ge, B.Z., Sato, K., Wang, Z., Kurokawa, J., Tan, J.N., Huang, K., Fu, J.S., Wang, X.M., Yamaji, K., Nagashima, T., Li, J., Kajino, M., Carmichael, G.R., Wang, Z.F., 2021. Insights into seasonal variation of wet deposition over southeast Asia via precipitation adjustment from the findings of MICS-Asia III. Atmos. Chem. Phys. 21, 8709–8734. https://doi.org/10.5194/acp-21-8709-2021.

Jiang, C.M., Yu, W.T., Ma, Q., Xu, Y.G., Zou, H., Zhang, S.C., Sheng, W.P., 2013. Atmospheric organic nitrogen deposition: analysis of nationwide data and a case study in Northeast China. Environ. Pollut. 182, 430–436. https://doi.org/10.1016/j.envpol.2013.08.003.

Jung, C.-G., Kim, S.-J., 2017. SWAT modeling of nitrogen dynamics considering atmospheric deposition and nitrogen fixation in a watershed scale. Agric. Sci. 08, 326–340. https://doi.org/10.4236/as.2017.84024.

Krotkov, N.A., Lamsal, L.N., Celarier, E.A., Swartz, W.H., Marchenko, S.V., Bucsela, E.J., Chan, K.L., Wenig, M., Zara, M., 2017. The version 3 OMI NO2 standard product. Atmos. Meas. Tech. 10, 3133–3149. https://doi.org/10.5194/amt-10-3133-2017.

Lamarque, J.F., Dentener, F., McConnell, J., Ro, C.U., Shaw, M., Vet, R., Bergmann, D., Cameron-Smith, P., Dalsoren, S., Doherty, R., Faluvegi, G., Ghan, S.J., Josse, B., Lee, Y.H., MacKenzie, I.A., Plummer, D., Shindell, D.T., Skeie, R.B., Stevenson, D.S., Strode, S., Zeng, G., Curran, M., Dahl-Jensen, D., Das, S., Fritzsche, D., Nolan, M., 2013. Multi-model mean nitrogen and sulfur deposition from the Atmospheric Chemistry and Climate Model Intercomparison Project (ACCMIP): evaluation of historical and projected future changes. Atmos. Chem. Phys. 13, 7997–8018. https://doi.org/10.5194/acp-13-7997-2013.

Li, M., Zhang, Q., Kurokawa, J.I., Woo, J.H., He, K., Lu, Z., Ohara, T., Song, Y., Streets, D.G., Carmichael, G.R., Cheng, Y., Hong, C., Huo, H., Jiang, X., Kang, S., Liu, F., Su, H., Zheng, B., 2017. MIX: A mosaic Asian anthropogenic emission inventory under the international collaboration framework of the MICS-Asia and HTAP. Atmos. Chem. Phys. 17, 935–963. https://doi.org/10.5194/acp-17-935-2017.

Li, R., Cui, L., Zhao, Y., Zhang, Z., Sun, T., Li, J., Zhou, W., Meng, Y., Huang, K., Fu, H., 2019. Wet deposition of inorganic ions in 320 cities across China: spatio-temporal variation, source apportionment, and dominant factors. Atmos. Chem. Phys. 19, 11043–11070. https://doi.org/10.5194/acp-19-11043-2019.

Li, R., Cui, L.L., Fu, H.B., Zhao, Y.L., Zhou, W.H., Chen, J.M., 2020. Satellite-based estimates of wet ammonium (NH4-N) deposition fluxes across China during 2011–2016 using a space-time ensemble model. Environ. Sci. Technol. 54, 13419–13428. https://doi.org/10.1021/acs.est.0c03547.

Liu, X.J., Duan, L., Mo, J.M., Du, E.Z., Shen, J.L., Lu, X.K., Zhang, Y., Zhou, X.B., He, C.N., Zhang, F.S., 2011. Nitrogen deposition and its ecological impact in China: an overview. Environ. Pollut. 159, 2251–2264. https://doi.org/10.1016/j.envpol.2010.08.002.

Liu, X.J., Xu, W., Pan, Y.P., Du, E.Z., 2015. Liu et al. suspect that Zhu et al. (2015) may have underestimated dissolved organic nitrogen (N) but overestimated total particulate N in wet deposition in China. Sci. Total Environ. 520, 300–301. https://doi.org/10.1016/j.scitotenv.2015.03.004.

Liu, L., Zhang, X.Y., Xu, W., Liu, X.J., Lu, X.H., Chen, D.M., Zhang, X.M., Wang, S.Q., Zhang, W.T., 2017. Estimation of monthly bulk nitrate deposition in China based on satellite NO2 measurement by the Ozone Monitoring Instrument. Remote Sens. Environ. 199, 93–106. https://doi.org/10.1016/j.rse.2017.07.005.

Liu, L., Yang, Y., Xi, R., Zhang, X., Xu, W., Liu, X., Li, Y., Liu, P., Wang, Z., 2021. Global wet-reduced nitrogen deposition derived from combining satellite measurements with output from a chemistry transport model. J. Geophys. Res. Atmos. 126. https://doi.org/10.1029/2020jd033977.

Liu, X., Zhang, Y., Han, W., Tang, A., Shen, J., Cui, Z., Vitousek, P., Erisman, J.W., Goulding, K., Christie, P., Fangmeier, A., Zhang, F., 2013. Enhanced nitrogen deposition over China. Nature 494, 459–462. https://doi.org/10.1038/nature11917.

Liu, X.J., Xu, W., Du, E.Z., Tang, A.H., Zhang, Y., Zhang, Y.Y., Wen, Z., Hao, T.X., Pan, Y.P., Zhang, L., Gu, B.J., Zhao, Y., Shen, J.L., Zhou, F., Gao, Z.L., Feng, Z.Z., Chang, Y.H., Goulding, K., Collett, J.L., Vitousek, P.M., Zhang, F.S., 2020. Environmental impacts of nitrogen emissions in China and the role of policies in emission reduction: reactive nitrogen issues in China. Philos. Trans. R. Soc. A Math. Phys. Eng. Sci. 378. https://doi.org/10.1098/rsta.2019.0324.

Lü, C., Tian, H., 2007. Spatial and temporal patterns of nitrogen deposition in China: synthesis of observational data. J. Geophys. Res. Atmos. 112. https://doi.org/10.1029/2006JD007990.

Neff, J.C., Holland, E.A., Dentener, F.J., McDowell, W.H., Russell, K.M., 2002. The origin, composition and rates of organic nitrogen deposition: a missing piece of the nitrogen cycle? Biogeochemistry 57, 99–136. https://doi.org/10.1023/A:1015791622742.

Pan, Y.P., Wang, Y.S., Tang, G.Q., Wu, D., 2012. Wet and dry deposition of atmospheric nitrogen at ten sites in Northern China. Atmos. Chem. Phys. 12, 6515–6535. https://doi.org/10.5194/acp-12-6515-2012.

Reinstorf, F., Binder, M., Schirmer, M., Grimm-Strele, J., Walther, W., 2005. Comparative assessment of regionalisation methods of monitored atmospheric deposition loads. Atmos. Environ. 39, 3661–3674. https://doi.org/10.1016/j.atmosenv.2005.03.006.

Tan, J., Fu, J.S., Dentener, F., Sun, J., Emmons, L., Tilmes, S., Sudo, K., Flemming, J., Jonson, J.E., Gravel, S., Bian, H., Davila, Y., Henze, D.K., Lund, M.T., Kucsera, T., Takemura, T., Keating, T., 2018. Multi-model study of HTAP II on sulfur and nitrogen deposition. Atmos. Chem. Phys. 18, 6847–6866. https://doi.org/10.5194/acp-18-6847-2018.

Tang, J., Xu, X., Ba, J., Wang, S., 2010. Trends of the precipitation acidity over China during 1992–2006. Chin. Sci. Bull. 55, 1800–1807. https://doi.org/10.1007/s11434-009-3618-1.

Vet, R., Artz, R.S., Carou, S., Shaw, M., Ro, C.U., Aas, W., Baker, A., Bowersox, V.C., Dentener, F., Galy-Lacaux, C., Hou, A., Pienaar, J.J., Gillett, R., Forti, M.C., Gromov, S., Hara, H., Khodzher, T., Mahowald, N.M., Nickovic, S., Rao, P.S.P., Reid, N.W., 2014. A global assessment of precipitation chemistry and deposition of sulfur, nitrogen, sea salt, base cations, organic acids, acidity and pH, and phosphorus. Atmos. Environ. 93, 3–100. https://doi.org/10.1016/j.atmosenv.2013.10.060.

Vitousek, P.M., Aber, J.D., Howarth, R.W., Likens, G.E., Matson, P.A., Schindler, D.W., Schlesinger, W.H., Tilman, D.G., 1997. Human alteration of the global nitrogen cycle: sources and consequences. Ecol. Appl. 7, 737–750. https://doi.org/10.1890/1051-0761(1997)007[0737, HAOTGN]2.0.CO;2.

Vivanco, M.G., Theobald, M.R., Garcia-Gomez, H., Garrido, J.L., Prank, M., Aas, W., Adani, M., Alyuz, U., Andersson, C., Bellasio, R., Bessagnet, B., Bianconi, R., Bieser, J., Brandt, J., Briganti, G., Cappelletti, A., Curci, G., Christensen, J.H., Colette, A., Couvidat, F., Cuvelier, C., D'Isidoro, M., Flemming, J., Fraser, A., Geels, C., Hansen, K.M., Hogrefe, C., Im, U., Jorba, O., Kitwiroon, N., Manders, A., Mircea, M., Otero, N., Pay, M.T., Pozzoli, L., Solazzo, E., Tsyro, S., Unal, A., Wind, P., Galmarini, S., 2018. Modeled deposition of nitrogen and sulfur in Europe estimated by 14 air quality model systems: evaluation, effects of changes in emissions and implications for habitat protection. Atmos. Chem. Phys. 18, 10199–10218. https://doi.org/10.5194/acp-18-10199-2018.

Walker, J.T., Dombek, T.L., Green, L.A., Gartman, N., Lehmann, C.M.B., 2012. Stability of organic nitrogen in NADP wet deposition samples. Atmos. Environ. 60, 573–582. https://doi.org/10.1016/j.atmosenv.2012.06.059.

Walker, J.T., Beachley, G., Amos, H.M., Baron, J.S., Bash, J., Baumgardner, R., Bell, M.D., Benedict, K.B., Chen, X., Clow, D.W., Cole, A., Coughlin, J.G., Cruz, K., Daly, R.W., Decina, S.M., Elliott, E.M., Fenn, M.E., Ganzeveld, L., Gebhart, K., Isil, S.S., Kerschner, B.M., Larson, R.S., Lavery, T., Lear, G.G., Macy, T., Mast, M.A., Mishoe, K., Morris, K.H., Padgett, P.E., Pouyat, R.V., Puchalski, M., Pye, H.O.T., Rea, A.W., Rhodes, M.F., Rogers, C.M., Saylor, R., Scheffe, R., Schichtel, B.A., Schwede, D.B., Sexstone, G.A., Sive, B.C., Echeverria, R.S., Templer, P.H., Thompson, T., Tong, D., Wetherbee, G.A., Whitlow, T.H., Wu, Z., Yu, Z., Zhang, L., 2019. Toward the improvement of total nitrogen deposition budgets in the United States. Sci. Total Environ. 691, 1328–1352. https://doi.org/10.1016/j.scitotenv.2019.07.058.

Wang, Z.F., Xie, F.Y., Sakurai, T., Ueda, H., Han, Z.W., Carmichael, G.R., Streets, D., Engardt, M., Holloway, T., Hayami, H., Kajino, M., Thongboonchoo, N., Bennet, C., Park, S.U., Fung, C., Chang, A., Sartelet, K., Amann, M., 2008. MICS-Asia II: model intercomparison and evaluation of acid deposition. Atmos. Environ. 42, 3528–3542. https://doi.org/10.1016/j.atmosenv.2007.12.071.

Wen, Z., Xu, W., Li, Q., Han, M., Tang, A., Zhang, Y., Luo, X., Shen, J., Wang, W., Li, K., Pan, Y., Zhang, L., Li, W., Collett Jr., J.L., Zhong, B., Wang, X., Goulding, K., Zhang, F., Liu, X., 2020. Changes of nitrogen deposition in China from 1980 to 2018. Environ. Int. 144, 106022. https://doi.org/10.1016/j.envint.2020.106022.

Xu, W., Luo, X.S., Pan, Y.P., Zhang, L., Tang, A.H., Shen, J.L., Zhang, Y., Li, K.H., Wu, Q.H., Yang, D.W., Zhang, Y.Y., Xue, J., Li, W.Q., Li, Q.Q., Tang, L., Lu, S.H., Liang, T., Tong, Y.A., Liu, P., Zhang, Q., Xiong, Z.Q., Shi, X.J., Wu, L.H., Shi, W.Q., Tian, K., Zhong, X.H., Shi, K., Tang, Q.Y., Zhang, L.J., Huang, J.L., He, C.E., Kuang, F.H., Zhu, B., Liu, H., Jin, X., Xin, Y.J., Shi, X.K., Du, E.Z., Dore, A.J., Tang, S., Collett, J.L., Goulding, K., Sun, Y.X., Ren, J., Zhang, F.S., Liu, X.J., 2015. Quantifying atmospheric nitrogen deposition through a nationwide monitoring network across China. Atmos. Chem. Phys. 15, 12345–12360. https://doi.org/10.5194/acp-15-12345-2015.

Xu, W., Zhang, L., Liu, X.J., 2019. A database of atmospheric nitrogen concentration and deposition from the nationwide monitoring network in China. Sci. Data 6, 51. https://doi.org/10.1038/s41597-019-0061-2.

Yoshioka, M., Regayre, L.A., Pringle, K.J., Johnson, J.S., Mann, G.W., Partridge, D.G., Sexton, D.M.H., Lister, G.M.S., Schutgens, N., Stier, P., Kipling, Z., Bellouin, N., Browse, J., Booth, B.B.B., Johnson, C.E., Johnson, B., Mollard, J.D.P., Lee, L., Carslaw, K.S., 2019. Ensembles of global climate model variants designed for the quantification and constraint of uncertainty in aerosols and their radiative forcing. J. Adv. Model. Earth Syst. 11, 3728–3754. https://doi.org/10.1029/2019MS001628.

Yu, G., Jia, Y., He, N., Zhu, J., Chen, Z., Wang, Q., Piao, S., Liu, X., He, H., Guo, X., Wen, Z., Li, P., Ding, G., Goulding, K., 2019. Stabilization of atmospheric nitrogen deposition in China over the past decade. Nat. Geosci. 12, 424–429. https://doi.org/10.1038/s41561-019-0352-4.

Zhang, Y., Song, L., Liu, X.J., Li, W.Q., Lü, S.H., Zheng, L.X., Bai, Z.C., Cai, G.Y., Zhang, F.S., 2012. Atmospheric organic nitrogen deposition in China. Atmos. Environ. 46, 195–204. https://doi.org/10.1016/j.atmosenv.2011.09.080.

Zhao, Y.H., Zhang, L., Chen, Y.F., Liu, X.J., Xu, W., Pan, Y.P., Duan, L., 2017. Atmospheric nitrogen deposition to China: a model analysis on nitrogen budget and critical load exceedance. Atmos. Environ. 153, 32–40. https://doi.org/10.1016/j.atmosenv.2017.01.018.

Zhu, J., He, N., Wang, Q., Yuan, G., Wen, D., Yu, G., Jia, Y., 2015. The composition, spatial patterns, and influencing factors of atmospheric wet nitrogen deposition in Chinese terrestrial ecosystems. Sci. Total Environ. 511, 777–785. https://doi.org/10.1016/j.scitotenv.2014.12.038.